**Title**

Complement proteins regulating macrophage polarisation on biomaterials

**Authors**

N. Araújo-Gomes[1,2*], F. Romero-Gavilán[1*&], Y. Zhang[3*], C. Martinez-Ramos[2], F. Elortza[4], M. Azkargorta[4], J.J. Martín de Llano[5], M. Gurruchaga[6], I. Goñi[6], J.J.J.P. van den Beucken[3], J. Suay[1]

[1] Departamento de Ingeniería de Sistemas Industriales y Diseño. Universitat Jaume I, Av. Vicent-Sos Baynat s/n. Castellón 12071. Spain.

[2] Department of Medicine. Universitat Jaume I, Av. Vicent-Sos Baynat s/n. Castellón 12071. Spain.

[3] Department of Biomaterials, PO Box 9101, 6500 HB Radboudumc, Nijmegen, TheNetherlands.

[4] Proteomics Platform, CIC bioGUNE, CIBERehd, ProteoRed-ISCIII, Bizkaia Science and Technology Park, 48160 Derio, Spain.

[5] Department of Pathology and Health Research Institute of the Hospital Clínico (INCLIVA), Faculty of Medicine and Dentistry, University of Valencia, 46010 Valencia, Spain

[6] Facultad de Ciencias Químicas. Universidad del País Vasco. P. M. de Lardizábal, 3. San Sebastián 20018. Spain.

[*]Co-authorship.

[&]Corresponding author: Francisco Romero-Gavlián

E-mail: gavilan@uji.es

Telephone number: +34964728773

**Abstract**

One of the events occurring when a biomaterial is implanted in an host is the protein deposition onto its surface, which might regulate cell responses. When a biomaterial displays a compromised biocompatibility, distinct complement pathways can be activated to produce a foreign body reaction. In this article, we have designed different types of biomaterial surfaces to study the inflammation process. Here, we used different concentrations of (3-glycidoxypropyl)-trimethoxysilane (GPTMS), an organically-modified alkoxysilane as a precursor for the synthesis of various types of sol-gel materials functionalizing coatings for titanium implants to regulate biological responses. Our results showed that increasing GPTMS concentration slightly enhanced the osteogenic potential of MC3T3-E1 cells *in vitro*, which seems linked to upregulation of TGF-β expression. Moreover, greater GPTMS surface concentrations induced greater secretion of TNF-α and IL-10 on RAW 264.7 macrophages. When implanted into rabbit tibia, osseointegration decreased with higher GPTMS concentrations. Interestingly, higher deposition of complement-related proteins C-reactive protein (CRP) and ficolin-2 (FCN2), two main activators of distinct complement pathways, was observed. Taking all together, inflammatory potential increase seems to be GPTMS concentration-dependent. Our results show that a greater adsorption of complement proteins can condition macrophage polarization.

**Keywords:**

Complement system; immune response; proteomics; dental implants; hybrid sol-gel; macrophage plasticity

## 1. Introduction

Bone healing and recovery after orthopaedic, spinal, and dental surgical procedures are the prime concerns for surgeons and patients. Researchers are still seeking for improvements in clinical performance to assure complete post-trauma bone healing in the shortest possible time. The need to find these improvements drives the development of biomaterials with bioactive properties, capable of stimulating bone growth and biodegradation [1].

Hybrid silica sol-gel materials belonging to the second generation of bioglasses have unique physicochemical properties that make them ideal candidates for bone biomaterials [2]. By applying sol-gel as a coating to implants, the desired bioactive properties are obtained; additionally, these coatings are biocompatible, biodegradable, and able to release silica compounds in $Si(OH)_4$ form. Silica is involved in bone metabolism, and enhances and promotes tissue mineralisation [3]. As such, the release of $Si(OH)_4$ confers silica hybrid sol-gels their osteoinductive properties [4]. The application of sol-gels as coatings, in particular on titanium implants, is increasingly used in the field of dental implantology [5,6]. Moreover, the versatility of the sol-gel techniques enables the preparation of coatings with control over their degradation kinetics, which renders these materials attractive release vehicles.

(3-Glycidoxypropyl) trimethoxysilane (GPTMS) is an organically modified alkoxysilane used as a precursor in the synthesis of sol-gel materials. It is non-cytotoxic, and the epoxy ring in its structure allows to functionalise the biomaterial network and modify its physicochemical properties [7]. Furthermore, the epoxy ring facilitates the incorporation of osteogenic or antibacterial drugs into the sol-gel network by covalent bonding [1]. Consequently, GPTMS-coated implants can be bioactivated with the desired signals to enhance biological performance. Nevertheless, despite the promising *in vitro* results [5], some sol-gels developed using GPTMS as a precursor demonstrated *in vivo* biocompatibility issues [8,9].

One of the main reasons for this discrepancy might be the lack of correlation between methods used for *in vitro* and *in vivo* evaluation of biomaterials [10]. Thus, further research into protein adhesion onto biomaterial surfaces becomes even more important for the development of improved formulations. The adhered proteins, depending on their type, conformation and quantity, might be responsible for cellular activation cascades and the subsequent cell behaviour, defining both *in vitro* and *in vivo* outcomes [11].

Biomaterials interact with their surroundings at several levels of biological organisation from the moment they are implanted, and come into contact with bodily fluids, such as

blood. The protein–implant interface triggers the activation of coagulation cascades, immune cell migration and complement system pathways. Together, this initiates the natural inflammation processes in response to a foreign body [12] as well as the bone regenerative processes after implantation. The first proteins adsorbing onto the surface can vary in type, number, and conformation (caused by competitive displacement; Vroman effect), depending on protein–protein and protein–surface interactions [13].

An activation of immune cells by these proteins is required for appropriate bone healing. The surface-adsorbed proteins participate in processes including clot formation, tissue granulation and cell recruitment, in a coordinated manner, with direct cross-talk between the osteogenic and immune cells [14].The interplay between immunology systems and bone forming cells is critical for osseointegration and to understand microenvironmental and cellular cues [15]. Specifically the role of macrophages has recently been recognized as critical for bone homeostasis, directly affecting the cross-talk between osteoblasts and osteoclasts [16,17].

These plastic cells, in response to extracellular signals and/or interaction with proteins, can adopt two main sub-phenotypes: pro-inflammatory M1 and anti-inflammatory M2 [18]. Emerging evidence indicates that the predominance of the M1 phenotype after implantation leads to chronic inflammation, compromising bone regeneration [19]. This can be related to the type and conformation of proteins attached to the material surface immediately after implantation. On the other hand, the M2 macrophage phenotype, known as a “reparative” phenotype, is described to have a pro-angiogenic character on tissue growth and development by secreting anti-inflammatory cytokines and osteoinductive molecules. M2a and M2c subsets, in particular, are suggested to have key roles in angiogenesis and vessel growth, enhancing endothelial cell sprouting and anastomosis through the secretion of PDGF-BB (M2a) and MMP9 (M2c) [20].

We here aimed to characterise complement protein adsorption to three sol-gel coatings made using different concentrations of GPTMS (0%, 35%, and 100%). Further, we analysed *in vitro* response to these materials using mouse osteoblastic cells MC3T3-E1 and mouse RAW264.7 macrophages. Finally, the *in vivo* effects of these compositions and correlations between the *in vivo* and *in vitro* results were examined.

## 2. Materials and Methods

### *2.1. Substrate*

Ti discs (12 mm in diameter, 1-mm thick) were made from a bar of commercially available, pure, grade-4 Ti (Ilerimplant-GMI S.L., Lleida, Spain) and submitted to sandblasting, acid-etching treatment (SAE). The discs were abraded with 4-μm aluminium oxide particles and acid-etched by submersion in sulfuric acid for 1 h. They were then washed with acetone, ethanol and 18.2-Ω purified water (20 min in each liquid) in an ultrasonic bath and dried under vacuum. Finally, all Ti discs were sterilised using UV radiation.

### *2.2. Sol-gel synthesis and sample preparation*

To obtain the hybrid silica coatings, the sol-gel method was used. The synthesis was performed using alkoxysilanes methyltrimethoxysilane (MTMOS), 3-glycidoxypropyl-trimethoxysilane (GPTMS) and tetraethyl orthosilicate (TEOS), purchased from Sigma-Aldrich (St. Louis, MO, USA). These precursors were combined in three distinct molar proportions to obtain the different compounds: 70 % MTMOS: 30 % TEOS (70M30T), 35 % MTMOS: 35 % GPTMS: 30 % TEOS (35M35G30T) and 100 % GPTMS (100G). 2-propanol (Sigma-Aldrich, St. Louis, MO, USA) was used as a solvent at a volume ratio (alcohol to siloxane) of 1:1. Hydrolysis of alkoxysilanes was carried out by adding (at a rate of a drop per second) the corresponding stoichiometric amount of acidified aqueous solution 0.1 M $HNO_3$ (Panreac, Barcelona, Spain). The solution was stirred for 1 h and then left to rest for 1 h. The samples were prepared immediately afterwards. SAE-Ti discs were used as a substrate. The coating was performed employing a dip coater (KSV instrument-KSV DC). Discs were immersed in a sol-gel solution at a speed of 60 cm $min^{-1}$, left for 1 min, and removed at a 100 cm $min^{-1}$. Finally, 70M30T and 35M30G30T samples were cured for 2 h at 80 °C, and 100G samples, for 2 h at 140 °C.

### *2.3. Physicochemical characterisation of coated titanium discs*

The coatings were examined using scanning electron microscopy (SEM), employing the Leica-Zeiss LEO equipment under vacuum (Leica, Wetzlar, Germany). Platinum sputtering was utilised to make the materials more conductive. The material roughness was analysed using a mechanical profilometer Dektack 6M (Veeco Instruments, Plainview, NY, USA). Two coated discs of each composition were tested. Three measurements were performed for each disc to obtain the average values of the Ra parameter. The contact angle was measured using an automatic contact angle meter OCA 20 (DataPhysics Instruments, Filderstadt, Germany). Aliquots of 10 μL of ultrapure

water were deposited on the disc surfaces at a dosing rate of 27.5 μL $s^{-1}$ at 25 °C. Contact angles were determined using the SCA 20 software. Six discs of each material were studied, after depositing two drops on each disc.

### *2.4. In vitro assays*

#### *2.4.1. Cell culture*

MC3T3-E1 (mouse calvaria osteosarcoma cell line) and RAW 264.7 (mouse murine macrophage cell line) were cultured on the coated titanium discs at a concentration of 1 × $10^4$ cells $well^{-1}$, in 24-well culture plates (Thermo Fisher Scientific, Waltham, MA, USA). The culture medium for both cell lines contained DMEM with phenol red (Gibco-Life Technologies, Grand Island, NY, USA), 1 % of 100× penicillin/streptomycin (Biowest Inc., Riverside, KS, USA) and 10 % of fetal bovine serum (FBS) (Gibco-Life Technologies). After incubation for 24 hours at 37 °C in a humidified (95 %) atmosphere with 5 % $CO_2$, the MC3T3-E1 cell-line medium was replaced with an osteogenic medium composed of DMEM with phenol red 1×, 1 % penicillin/streptomycin, 10 % FBS, 1 % ascorbic acid (5 mg $mL^{-1}$) and 0.21 % β-glycerol phosphate and incubated again under the same conditions. The culture medium was changed every 48 hours. In parallel, MC3T3-E1 cells were allowed to differentiate for 7 and 14 days for RNA isolation.

The medium from RAW 264.7 cell culture on the titanium discs was harvested at 24 and 72 h to measure IL1-β, TNF-α, IL-10 and TGF-β content using ELISA, and the cells were fixed for immunostaining. In parallel, cells at the same concentration (1 × $10^4$ cells) incubated without biomaterials were used as a control of culture conditions.

#### *2.4.2. Cytotoxicity*

Materials were incubated with cell medium for 24 h. The biomaterial cytotoxicity was evaluated after 24 h of contact of MC3T3-E1 cells with the medium extracted after the initial incubation, using spectrophotometry. The CellTitter 96 Proliferation Assay (Promega®, Madison, WI, USA) was employed to measure cell viability after 24-h incubation, following manusfacturer's instructions. The medium with no cells was used a negative control, and latex, known to be toxic to the cells, was used as a positive control.

#### *2.4.3. Alkaline phosphatase (ALP) activity*

The conversion of p-nitrophenylphosphate (p-NPP) to p-nitrophenol was used to assess ALP activity, as previously described [9]. The results were presented as mmol of p-nitrophenol/hour (mmol PNP $h^{-1}$). The data were expressed as ALP activity normalised to the total protein content (μg $μL^{-1}$) obtained using Pierce BCA assay kit (Thermo Fisher Scientific, Waltham, MA, USA) after 7 and 14 days of cell culture.

### 2.4.4. *RNA isolation and cDNA synthesis*

Total RNA isolation and subsequent cDNA synthesis were adapted from the protocol described in [21]. Briefly, for each sample, approximately 1 µg of total RNA was converted to cDNA using PrimeScript RT Reagent Kit (Perfect Real Time) (TAKARA Bio Inc., Shiga, Japan). The resulting cDNA was diluted in DNase-free water to a concentration suitable for reliable RT-PCR analysis.

### *2.4.5. Osteogenic expression*

The primers for assessing the expression levels of the markers ALP, IL-6, COL I and TGF-β were designed using specific DNA sequences for these genes available from NCBI (https://www.ncbi.nlm.nih.gov/nuccore), employing the PRIMER3plus software tool (http://www.bioinformatics.nl/cgi-bin/primer3plus/primer3plus.cgi). The expression levels, shown in Table 1, were measured using primers purchased from Life Technologies S.A. (Gaithersburg, MD).

**Table 1**: Primers used for qRT-PCR

| Gene | Forward sense | Reversed sense |
|---|---|---|
| **IL-6** | AGTTGCCTTCTTGGGACTGA | TCCACGATTTCCCAGAGAAC |
| **COLI** | CCTGGTAAAGATGGTGCC | CACCAGGTTCACCTTTCGCACC |
| **TGF-β** | TTGCTTCAGCTCCACAGAGA | TGGTTGTAGAGGGCAAGGAC |
| **GADPH** | TGCCCCCATGTTTGTGATG | TGGTGGTGCAGGATGCATT |

GADPH was used as a housekeeping gene to normalise the data obtained from the qRT-PCR and calculate the relative fold-change between different conditions. qPCR reactions were carried out using SYBR Premix Ex Taq (Tli RNase H Plus) (TAKARA), in a StepOne Plus™ Real-Time PCR System (Applied Biosystems, Foster City, California, USA). The cycling parameters were as follows: an initial denaturation step at 95 °C for 30 s; followed by 95 °C for 5 s and 60 °C for 34 s for 40 cycles. The final melt-curve stage comprised a cycle of 95 °C for 15 s and 60 °C for 60 s.

### *2.4.6. Immunocytochemistry double staining*

RAW 264.7 cultures were fixed in 4 % paraformaldehyde for 10 min (Sigma-Aldrich, St. Louis, MO, USA) and washed 5 times in 1x PBS. The samples were blocked in 1x PBS containing 0.5 % BSA (Sigma-Aldrich, St. Louis, MO, USA) and 1 % Triton X-100 (Sigma-Aldrich, St. Louis, MO, USA). They were incubated with donkey anti-mouse CD206

primary antibody (Abcam, Cambridge, UK) diluted 1:250 in PBS containing 0.5 % BSA and 0.5 % Tween-20 (Sigma-Aldrich), overnight at 4 °C. The discs were then washed 5 times in 1x PBS and incubated with a mixture of secondary antibodies composed of Goat anti-Donkey Biotin (Jackson ImmunoResearch Europe, Ltd., Cambridgeshire, UK) 1:500 and Streptavidin Alexa Fluor 647 1:500 (Thermo Fisher Scientific, US) for 1 h at room temperature. Cells were washed 5 times again with 1x PBS with 0.5 % Triton X-100 and incubated with the primary antibody IL7-R (Santa Cruz Biotechnology, Dallas, TX, USA) at 4 °C overnight. After 5 more washes with 1x PBS with 0.5 % Triton X-100, the discs were incubated with the secondary antibody Goat anti-Rabbit Alexa Fluor 488 (Thermo Fisher Scientific, Waltham, MA, USA) for 1 h at room temperature. After the next 5 washes with 1x PBS with 0.5 % Triton X-100, the discs were incubated with DAPI (Roche, Basel, Switzerland) for another hour to stain the cell nuclei.

The discs were then removed from the wells, mounted on coverslipped slides with mounting medium (4.8 % poly(vinyl alcohol-co-vinyl acetate); 12 % glycerol; 0.2M Tris-HCl; 0.02 % sodium azide) and stored at 4 °C for the fluorescence microscopy analysis. All images were captured using the same exposure time.

#### *2.4.7. Cytokine quantification*

The ELISA kits for TNF-α, IL1-β, IL-10 and TGF-β (Thermo Fisher Scientific, Waltham, MA, USA) were employed to quantify the proteins produced by RAW 264.7 cells cultured on each of the materials tested (following manufacturer's instructions).

### *2.5. Proteomic analysis*

Proteomic analysis was performed as described previously [22], with minor variations. Briefly, the eluted protein was in-solution digested, following the FASP protocol established by Wisnewski *et al.* [23] and loaded onto a nanoACQUITY UPLC System connected online to an SYNAPT G2-Si MS System (Waters, Milford, MA, USA). Each material was analysed in quadruplicate. The statistical protein analysis was carried out using Progenesis software (Nonlinear Dynamics, Newcastle, UK). The functional annotation of the identified differential proteins was performed using the DAVID GO annotation programme (https://david.ncifc rf.gov/). Proteins were quantified based on the intensity of their three most abundant peptides, when available. Proteins with analysis of variance (ANOVA) $p < 0.05$ and a ratio higher than 1.3 in either direction were considered significantly different. Each material was analysed in quadruplicate.

### *2.6. In vivo experimentation*

The *in vivo* experimentation was performed as described in [22]. Briefly, the *in vivo* procedures and histological evaluation of the three tested materials, 70M30T, 35M35G30T and 100G, were carried out using the tibia of New Zealand rabbits (Oryctolagus cuniculus) as the experimental model. All the experiments were conducted in accordance with the protocols of the Ethical Committee of the Valencia Polytechnic University (Spain), the European guidelines and legal conditions described in R. D. 223/1988 of March 14th and the Order of October 13th, 1988, of the Spanish Government on the protection of animals used for experimentation and other scientific purposes. The dental implants, supplied by Ilerimplant S.L. (Lleida, Spain), were the Frontier model (3.75-mm diameter and 8-mm length) with SAE surface treatment. Four implants per animal were used, two control non-coated titanium implants on one tibia and two coated implants (of each material) on the other. The implantation period was 2 weeks. The samples for histological examination were embedded in methyl methacrylate using EXAKT technique (EXAKT Technologies, Inc., Oklahoma, USA). The slides were stained with Stevenel's blue and van Gieson's picro-fuchsin, following the procedure described by Maniatopoulos et al. [24]. Digital images of the tissues were recorded using a brightfield Leica DM4000 B microscope and a DFC420 digital camera.

### *2.7. Statistical analysis*

Data were analysed using a one-way ANOVA combined with a Newman-Keuls multiple comparison post-hoc test where appropriate (GraphPad Prism; GraphPad Software, Inc., California, USA). P-values $\leqslant 0.05$ were considered statistically significant.

## 3. Results

### *3.1. Synthesis and physicochemical characterisation*

The different sol-gels were synthesised and applied as coatings on titanium surfaces. They were homogeneous and adhered well to the Ti discs. Different topographies were observed via SEM micrographs, showing coverage of the original SAE-Ti irregular surface (Fig. 1a-c). The morphological differences were concordant with the measured surface roughness (Ra values; Fig. 1d): surface roughness significantly decreased with increasing GPTMS precursor content in the sol-gel coating.

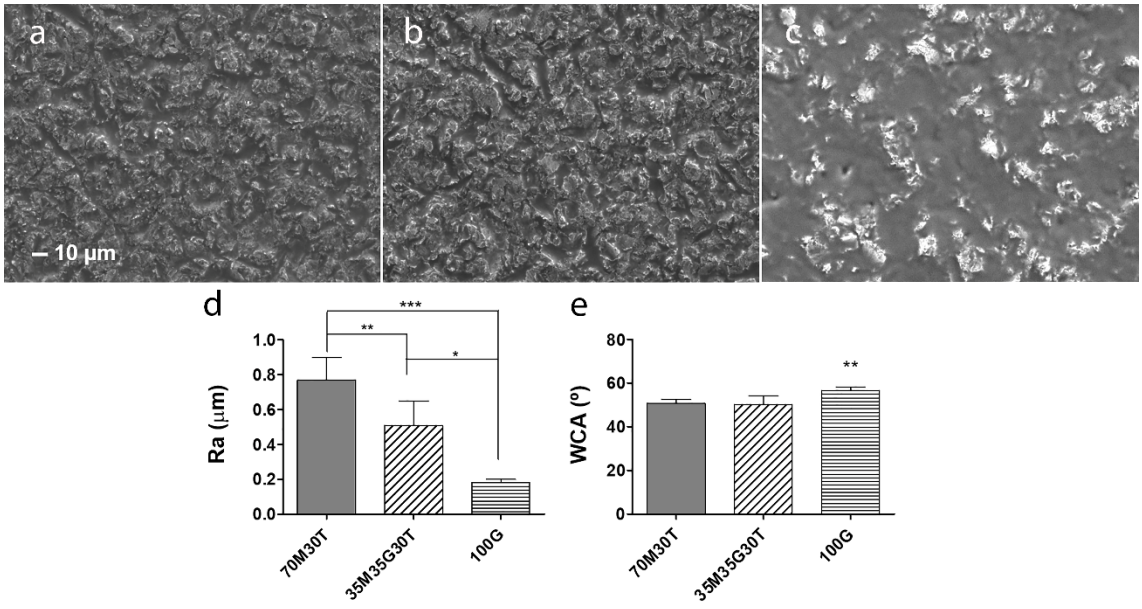


**Figure 1**. SEM micrographs of 70M30T (a), 35M35G30T (b) and 100G (c) sol-gel coated surfaces. Calibration bar, 10 µm. (d) Ra values for each formulation (n = 6) and (e) Wettability of substrates by water contact angle (WCA) measurements (n=6). Statistical analysis was performed using one-way ANOVA with Newman-Keuls post-hoc test. *, $P < 0.05$; **, $P < 0.01$; ***, $P < 0.001$.

The measured contact angles were 50.78 ± 1.82°, 50.39 ± 3.78° and 56.51 ± 1.69° for 70M30T, 35M35G30T and 100G coatings, respectively.

### *3.2. In vitro experimentation*

The 70M30T and 35M35G30T sol-gel coatings used in this study enhanced the cellular viability for osteoblastic MC3T3-E1 cells (Fig. 2a) when compared to positive controls. The osteogenic differentiation potential, assessed by measuring ALP activity, showed no apparent differences between the distinct sol-gel materials (Fig. 2b; $p \geq 0.05$).

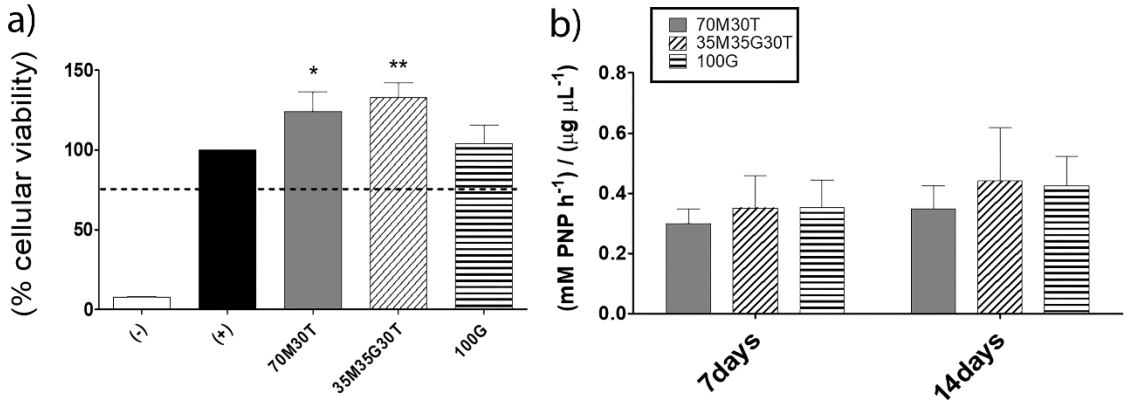


**Figure 2.** MC3T3-E1 *in vitro* assays. a) MC3T3-E1 cell survival assay. Cells in a well without a disc were used as a positive control, 100% cell viability – the dashed line represents the limit above which the material is considered cytotoxic. b) ALP activity (mM PNP $h^{-1}$) normalised to the total protein levels (µg $µL^{-1}$) in the MC3T3-E1 cells cultivated on titanium discs with the different formulations. Statistical analysis was performed using one-way ANOVA with Newman-Keuls post-hoc test. *, $P < 0.05$; **, $P < 0.01$.

TGF-β expression was significantly upregulated in the MCT3T3-E1 cells cultured on the sol-gel hybrid surfaces (in comparison with the SAE-Ti). Interestingly, the upregulation of this gene was found for the materials containing GPTMS (100G at 7 days and 35M35G30T at 14 days; Fig. 3).

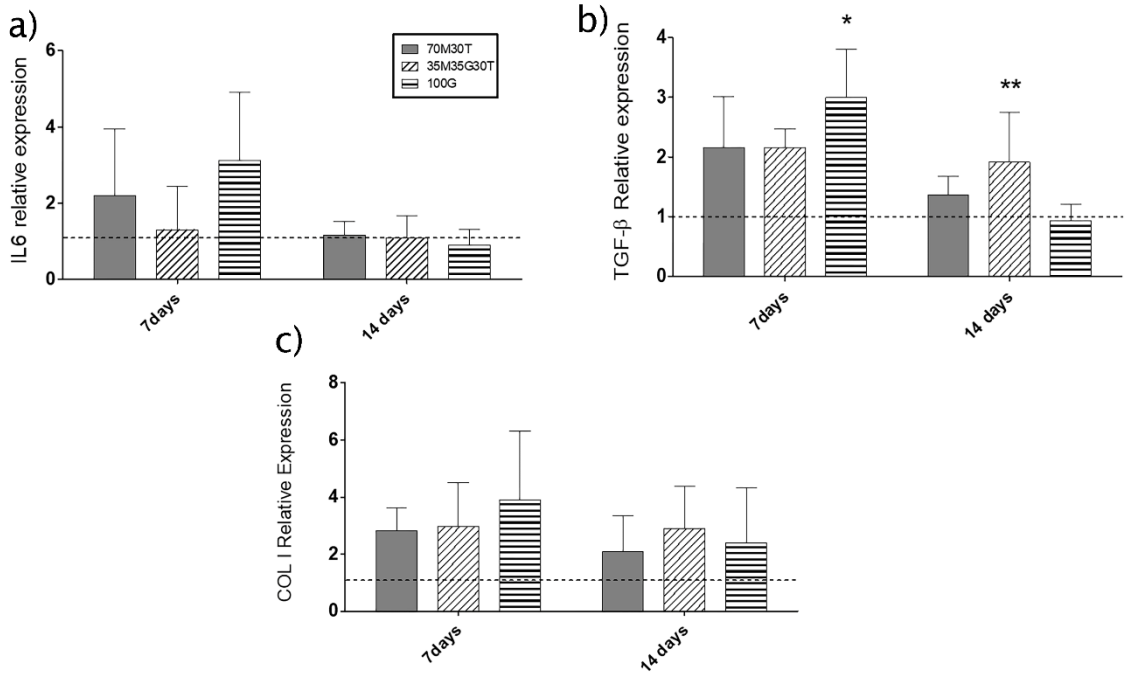


**Figure 3.** Gene expression of osteogenic markers a) IL6, b) TGF-β and c) COL-1 in MC3T3-E1 osteoblastic cells cultured on different formulations. Relative mRNA

expression was determined by RT-PCR after 7 and 14 days of culture. Statistical analysis was performed using one-way ANOVA with Newman-Keuls post-hoc test. *, $P < 0.05$; **, $P < 0.01$; ***, $P < 0.001$.

To evaluate the effect of different coatings on RAW264.7 macrophage polarization, pro- and anti-inflammatory cytokine secretion profiles were determined. The cytokine secretion profiles at 24h of culture were similar among coatings. After 72h, a significantly increased release of TNF-α (Fig. 4c; p-value < 0.001) and IL-10 (Fig. 4d; p-value < 0.001) was observed for macrophages cultured on the material with the highest concentration of GPTMS (100G). On the two coatings with lower concentrations of this precursor, the values of TNF-α release did not differ (Fig. 4c; p>0.05).

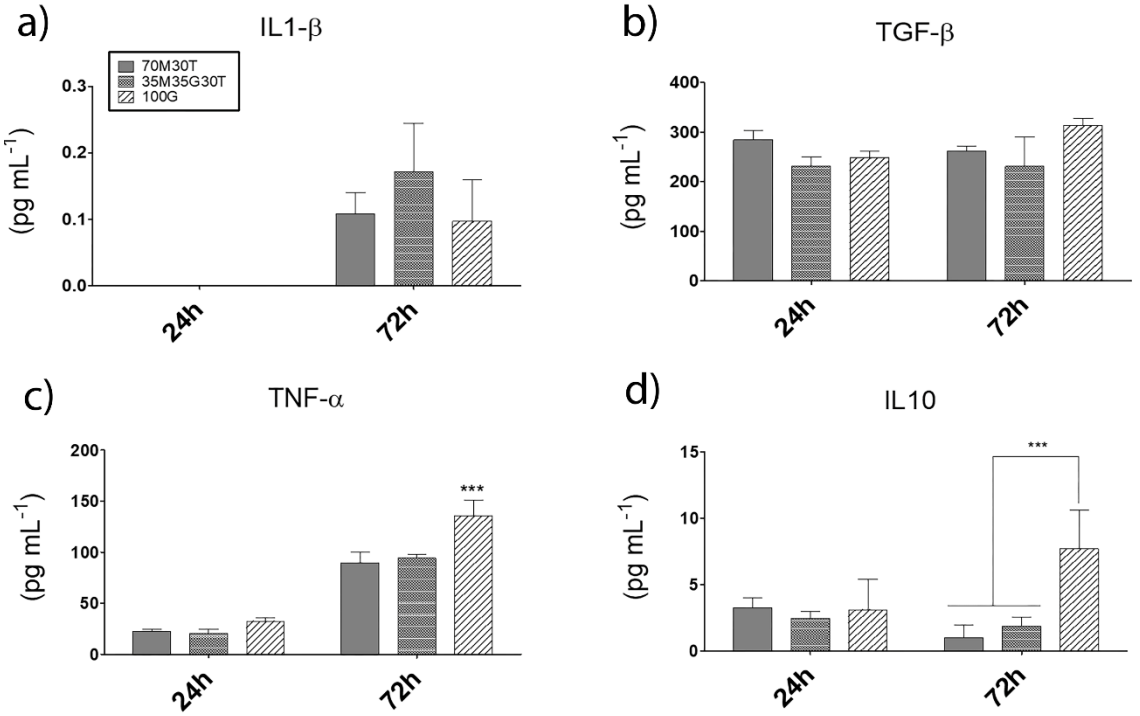


**Figure 4**. Cytokine expression. IL1-β (a), TGF-β (b), TNF-α (c) and IL10 (d) in RAW 264.7 macrophages at 24- and 72-h time points. Statistical analysis was performed using one-way ANOVA with Newman-Keuls post-hoc test. *, $P < 0.05$; **, $P < 0.01$; ***, $P < 0.001$.

M1 macrophage marker IL7-R showed increased fluorescent expression for macrophage cultures on the GPTMS materials at the 72-h time point compared to the material with no GPTMS (Fig. 5a′-c′; p-value < 0.001).No significant differences were found for CD206 fluorscent expression between materials. (Fig. 5a''-c''; p-value ≥ 0.05).

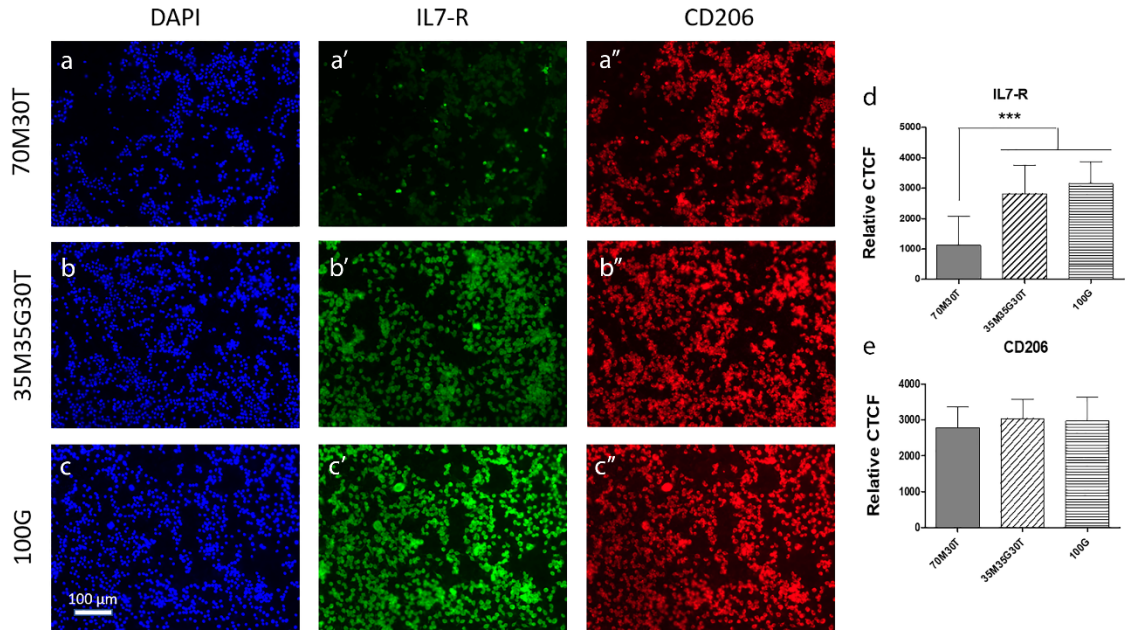


**Figure 5**. Immunostaining of macrophages cultured on the 70M30T, 35M35G30T and 100G sol-gel hybrid coatings, after 72 h. IL7-R (a′-c′) was used as a pro-inflammatory M1 marker and CD206 (a″-c″), the anti-inflammatory M2 marker. The relative corrected total cell fluorescence (CTCF) of these markers (d and e) was quantified using ImageJ. Statistical analysis was performed by one-way ANOVA with Newman-Keuls post-hoc test, *** $P < 0.001$.

### *3.3. In vivo experimentation*

Fig. 6 displays the histological results for the coatings employed. Three notable features were observed. The implant grooves on the cortical region into which the bone tissue penetrates were similar for 35M35G30T and 70M30T. This was less pronounced for the 100G sample. The spicules from the cortical, following the implant surface in the medullary cavity, were longer greater and more developed on 70M30T than on the other two formulations (approximately a half of the length on 35M35G30T and one-third on 100G).

The mean size of the multinucleated giant cells (contacting the implant or coating surface) on the medullary zone was smaller on the 70M30T samples (approximately 0.25 mm) in comparison with the other two materials (approximately 0.3 mm). Moreover, the density of giant cells covering the outline of titanium implant and coating (number of cells per length) was also lower on the 70M30T material (0.7 cells per mm) than on the other two formulations (1.3 cells per mm for 35M35G30T and 1 cell per mm for 100G).

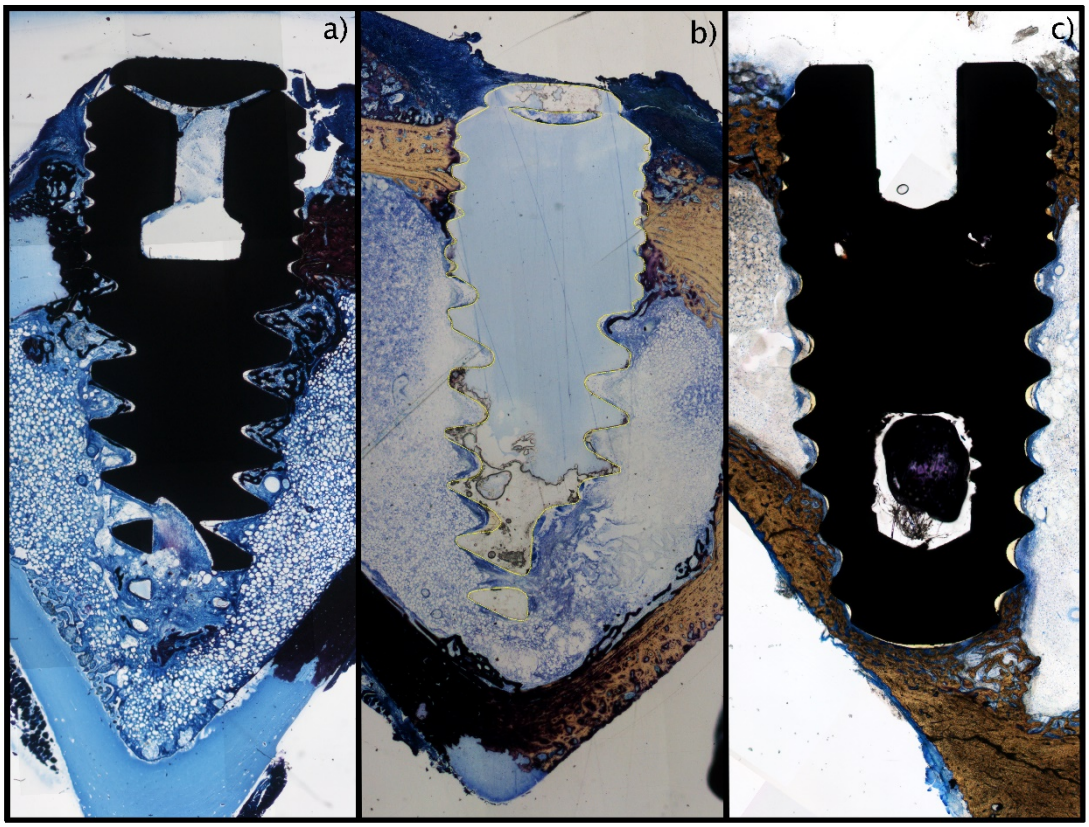


**Figure 6**. Microphotographs of titanium implants. Panoramic images of (a) 70M30T, (b) 35M35G30T and (c) 100G implants showing the cortical bone region and the medullary cavity. The implant grooves in (b) delimit the metal layer of the implant detached during the processing of the sample.

### *3.4. Proteomic analysis*

The eluted proteins analysed using LC-MS/MS and Progenesis QI software and subsequent DAVID analysis show some significant differences between the types and functions of the proteins adsorbed to the different materials tested. One hundred seventy-six proteins are identified as adsorbed commonly to the three formulations. Among this group, and after Progenesis comparative analysis, sixteen proteins are found to be directly associated with immune response processes, *i.e.* the complement system. These are significantly more adsorbed onto the materials made with GPTMS, with a tendency for an increased abundance on materials with more GPTMS (Supplementary table).

A significantly higher adsorption of FCN2 to the 100G material was seen in comparison with the other two materials (70-fold increase in comparison with the 70M30T and 8.5-fold increase in comparison with the 35M35G30T). CRP and FCN2 showed a tendency for increased attachment to the formulation with the highest concentration of GPTMS. The normalized abundance of proteins CRP, FCN2, CO3, CO5, C1q, that play a central

role on complement system pathway development is stated on Fig. 7. It is clear the greater adsorption of these onto the highest GPTMS content formulation.

At the same time, DAVID identifies SAMP as the protein prevalently associated with the materials with high GPTMS content. This pentraxin-family protein, sharing some traits with the CRP, is also involved in the processes of immune and acute inflammatory responses [25]. However, its effect on complement activation cascades is less clear than that of the CRP. The increase in the levels of VTNC and APOE on the GPTMS-coated materials is also worth mentioning (Supplementary table).

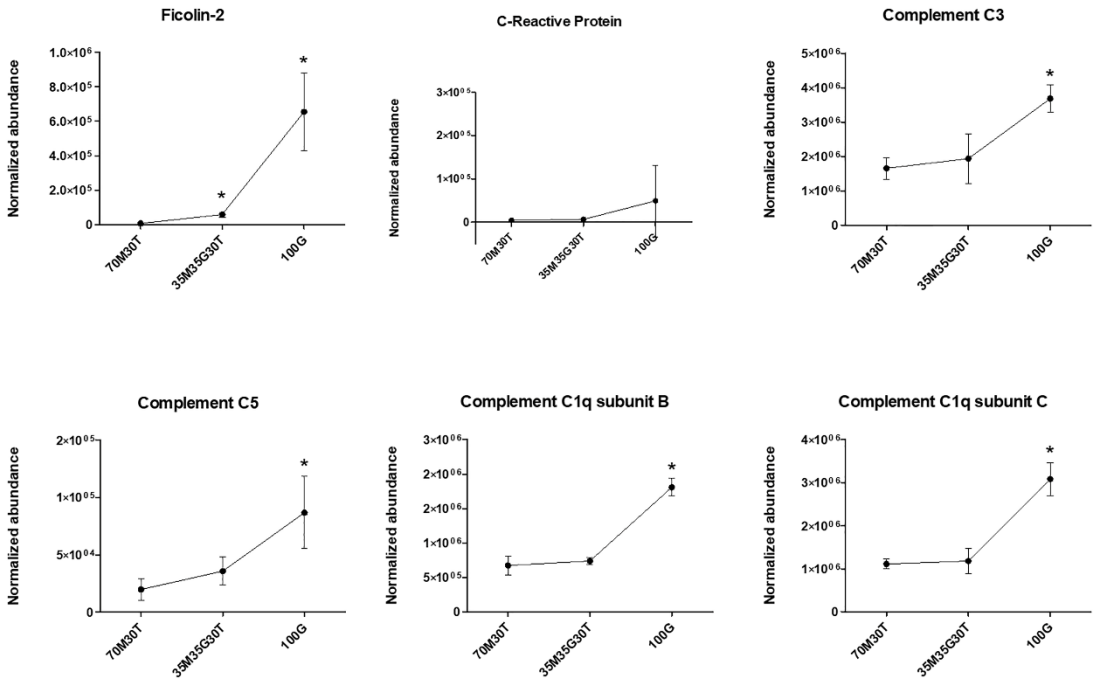


**Figure 7.** Normalized abundance of complement-related main proteins adsorbed to 70M30T, 35M35G30T and 100G. Statistical analysis was performed using one-way ANOVA with Newman-Keuls post-hoc test. * show significance when compared to the 70M30T coating. ANOVA, $P<0.05$.

## 4. Discussion

The urgent clinical need for orthopaedic biomaterial-based treatments is shifting the research in this field towards the design of so-called “bioactive” materials capable of interaction and integration in the biological microenvironment (*e.g.* molecules, cells) [26]. This interaction should be ideally modulated and guided through the evolution of materials with both osteoconductive and osteoinductive properties, leading ultimately to improved osseointegration [21]. As found in our previous studies, some of the here tested materials possess such intrinsic properties. However, certain processes, particularly those related to the material-induced immune response, can hamper the successful application of biomaterials in complex biological contexts [8,9]. First step in the design of new biomaterials with specific properties is to perform *in vitro* experimentation but the limitations of classical *in vitro* testing are widely recognised. However, the lack of correlation with the *in vivo* results has been largely disregarded [10]. Thus, there is a clear need to explore alternative assessment methodologies for biomaterial-based testing.

The use of hybrid silica sol-gel materials applied as coatings for dental implantation has been attracting increasing interest due to the intrinsic osteogenic properties of these formulations. This osteogenic potential depends on the degradation properties, i.e. the release of silica compounds in the $Si(OH)_4$ form, which can boost the osteoblastic behaviour in areas close to the coating [5]. 3-glycidoxypropyl-trimethoxysilane (GPTMS) is one of the organo-modified alkoxysilanes commonly employed in the development of hybrid materials [27] and is increasingly used in bone tissue engineering [28]. GPTMS has a characteristic epoxy ring susceptible to nucleophilic attack.

Here, we focused on the characterisation of the protein layer adsorbed onto materials with different concentrations of GPTMS and examined the correlations with *in vitro* and *in vivo* outcomes. We evaluated the osteogenic properties of this compound and examined the inflammatory effect of increasing concentrations of GPTMS; such increased GPTMS content might impair the biocompatibility of the coatings. The different chemical composition of the three formulations used in our experiments entails varying degrees of functionalisation of the surfaces. It was observed some clear morphological differences between the tested materials (Fig. 1), in which these distinct chemical compositions have proven to ultimately and naturally affect protein deposition on their surfaces.

*In vivo*, the 100G coating did not increase the osteogenic activity. Adding GPTMS to coating materials did not improve osteogenesis in those experiments. In fact, the bone spicules around these implants were shorter. However, the mean size and cell density of the multinucleated giant cells in contact with the coated implant were higher for both

GPTMS-coated samples; this might be associated with a strengthened immune response of the host. The formation of these cells requires an initial adhesion and is affected by the type of surface and the adsorbed blood proteins [29]. The appearance of foreign-body giant cells can inhibit the bone formation process and impair the material biocompatibility [30].

For the 100G material, our proteomic study showed an increase in the affinity of proteins with a direct role in the complement pathway processes, in comparison with the other two formulations. The significantly improved adsorption of FCN2 and CRP, identified by DAVID as main activators of distinct complement system pathways [31,32] (lectin and classical, respectively), shows that this formulation strengthens the inflammatory response. The rise in the affinity of complement proteins (CO3, CO5, C1QA, C1QB, CO7, C1R, C1S, CO8B and CO6) and the formation of C5b-9 membrane attack complex can be related to the increased deposition of these two activators. Within this cluster, CO3, CO5, CO6 and CO8G are common to the three pathways, participating in the termination step forming the C5b-9 membrane attack complex [33]. CO3 modulates the complement cascade activation and is a biomarker of inflammatory response to biomaterials [34]. CFAD is exclusive to the alternative pathway of the complement system; it is crucial for the cleavage of the lysine-arginine bond in the complement factor B [35,36]. Many of the complement proteins are activated in the host at the site of inflammation, forming convertases (namely C3 and C5 convertases) as the end-product. This results in the successive cleaving of the components, in a gain-and-loss manner, in an attempt to fight the pathogen or foreign body [33]. However, the increased abundance of proteins like VTNC and APOE might also result in a rise in the osteogenic potential. A study performed by our group has highlighted the bioactive potential of this type of coatings, associated with these two proteins [37]. However, at the time of increased cell inflammatory response, it is difficult to identify the specific role of these proteins in the regenerative processes.

ELISA analysis showed an increased secretion of TNF-α and IL-10 when the formulation 100G is used for macrophage culture. This data agrees with the results of the double staining, in which is observable an increased predominance of M1 macrophages on the coatings with GPTMS, showing a possible inflammatory potential for these coatings.

TNF-α release is typically associated with macrophage differentiation into the pro-inflammatory phenotype (M1). Interestingly, it has been reported that human CRP administered to rats induces macrophage polarisation to M1 and is associated with an increase in TNF-α release [38]. The release of IL-10, even though it is considered a M2 marker for human cells, is oppositely regulated on mice cells [39], and it is significantly increased on the 100G material. This might be due to the presence of the epoxy ring;

the macrophages might mistake it for lipopolysaccharide (LPS), as LPS also contains epoxy rings. It has been reported that the LPS increases the release of IL-10 on mouse cells [40,41]. Hence, we might be tempted to infer that the GPTMS causes macrophage differentiation into a pro-inflammatory M1 state not only via the TNF-α release but also by increasing the levels of IL-10. Although the M1 macrophages are necessary for the early inflammatory processes and wound healing, the increased secretion of TNF-α by these macrophages can impair bone formation. This cytokine is a potent factor of osteoclastogenesis and, at the same time, an inhibitor of osteoblastogenesis [42]. Wu *et al.* have reported that the predominance of the M1 phenotype on bone tissue may enhance the osteonecrosis through the liberation of TNF-α [43]. Hence, continuing high abundance of M1 macrophages might be associated with the worst *in vivo* outcome.

However, it is tempting to hypothesise that increased and immediate deposition of complement proteins on a surface affects the macrophage behaviour, to boost phagocytosis of the pathogens or foreign bodies [44,45]. The macrophage activation results in binding various complement proteins (C1q, MBL and even ficolins) to complement receptors on these cells. This modulates the cytokine production, the magnitude of the consequent immune response and pathogen opsonisation [46]. Complement proteins like anaphylatoxins C3a, C5a and the membrane attack complex C5b-9 are associated with macrophage induction into the inflammatory M1 phenotype [47,48]. The strength of immune response on the tested materials is also shown by the immunostaining, demonstrating discernible intensity differences for the M1 marker IL7-R. On the 100G formulation, the intensity of this marker was higher than on the other two materials.

The improved osteogenicity of GPTMS formulations, due to an increase in the abundance of vitronectin and APOE and a rise of osteogenic gene expression *in vitro*, is not clearly confirmed by the histological results. A possible reason for this disparity might be the significant immune response detected on this coating. The proteomic analysis shows that the proteins related to complement cascade activation are predominantly attached to this type of coating, and an increase in the macrophage-activated immune response is observed.

## 5. Conclusions

The increased adsorption of specific complement proteins and likely predominance of pro-inflammatory macrophage polarization here is related to the inferior *in vivo* performance of biomaterial surfaces containing different concentrations of GPTMS precursor. These data hence suggest an important role for complement proteins in determining the immune response to biomaterials.

Different complement pathways seem to be gradually activated in response to the increasing amounts of GPTMS, since an increased adsorption of FCN (lectin pathway activator) was observed on a GPTMS dose-dependent manner.

The results of this study are in agreement with our previous studies, highlighting the potential of proteomic analysis as an important tool for predicting *in vivo* outcomes. Moreover, the analysis of macrophage polarisation patterns on biomaterials might become a useful approach to correlation of *in vitro* assessment with *in vivo* outcome.


## Acknowledgements

This work was supported by MINECO [ MAT2017-86043-R ]; Universitat Jaume I [grant numbers Predoc/2014/25, UJI-B2017-37]; Basque Government [grant numbers IT611-13, Predoc/2016/1/0141]; University of the Basque Country [grant number UFI11/56]; CIC bioGUNE is supported by Basque Department of Industry, Tourism and Trade (Etortek and Elkartek programs), the Innovation Technology Department of the Bizkaia County; The ProteoRed-ISCIII (Grant PRB3 IPT17/0019); CIBERehd Network and Severo Ochoa Grant (SEV-2016-0644). Authors would like to thank Antonio Coso and Jaime Franco (GMI-Ilerimplant) for their inestimable contribution to this study, and Raquel Oliver, Jose Ortega (UJI), René van Rheden (Radboudumc), Vicent Cuijpers (Radboudumc) and Iraide Escobes (CIC bioGUNE) for their valuable technical assistance.

**References**


[1] D. Carboni, A. Pinna, L. Malfatti, P. Innocenzi, Smart tailoring of the surface chemistry in GPTMS hybrid organic–inorganic films, New J. Chem. 38 (2014) 1635–1640. doi:10.1039/C3NJ01385E.

[2] D. Arcos, M. Vallet-Regí, Sol-gel silica-based biomaterials and bone tissue regeneration., Acta Biomater. 6 (2010) 2874–88. doi:10.1016/j.actbio.2010.02.012.

[3] M.J. Juan-Díaz, M. Martínez-Ibáñez, I. Lara-Sáez, S. da Silva, R. Izquierdo, M. Gurruchaga, I. Goñi, J. Suay, Development of hybrid sol–gel coatings for the improvement of metallic biomaterials performance, Prog. Org. Coatings. 96 (2016) 42–51. doi:10.1016/j.porgcoat.2016.01.019.

[4] A.F. Khan, M. Saleem, A. Afzal, A. Ali, A. Khan, A.R. Khan, Bioactive behavior of silicon substituted calcium phosphate based bioceramics for bone regeneration, Mater. Sci. Eng. C. 35 (2014) 245–252. doi:10.1016/j.msec.2013.11.013.

[5] M. Martinez-Ibañez, M.J. Juan-Diaz, I. Lara-Saez, A. Coso, J. Franco, M. Gurruchaga, J. Suay Anton, I. Goñi, Biological characterization of a new silicon based coating developed for dental implants, J. Mater. Sci. Mater. Med. 27 (2016). doi:10.1007/s10856-016-5690-9.

[6] F. Romero-Gavilán, S. Barros-Silva, J. García-Cañadas, B. Palla, R. Izquierdo, M. Gurruchaga, I. Goñi, J. Suay, Control of the degradation of silica sol-gel hybrid coatings for metal implants prepared by the triple combination of alkoxysilanes, J. Non. Cryst. Solids. 453 (2016). doi:10.1016/j.jnoncrysol.2016.09.026.

[7] L. Gabrielli, L. Connell, L. Russo, J. Jiménez-Barbero, F. Nicotra, L. Cipolla, J.R. Jones, Exploring GPTMS reactivity against simple nucleophiles: chemistry beyond hybrid materials fabrication, RSC Adv. 4 (2014) 1841. doi:10.1039/c3ra44748k.

[8] N. Araújo-Gomes, F. Romero-Gavilán, A.M. Sanchez-Pérez, M. Gurruchaga, M. Azkargorta, F. Elortza, M. Martínez-Ibáñez, I. Iloro, J. Suay, I. Goñi, Characterization of serum proteins attached to distinct sol – gel hybrid surfaces, (2017) 1–9. doi:10.1002/jbm.b.33954.

[9] F. Romero-Gavilan, A.M. Sánchez-Pérez, N. Araújo-Gomes, M. Azkargorta, I. Iloro, F. Elortza, M. Gurruchaga, I. Goñi, J. Suay, Proteomic analysis of silica hybrid sol-gel coatings: a potential tool for predicting the biocompatibility of implants *in vivo*, Biofouling. 33 (2017) 676–689. doi:10.1080/08927014.2017.1356289.

[10] G. Hulsart-Billström, J.I. Dawson, S. Hofmann, R. Müller, M.J. Stoddart, M. Alini,

H. Redl, A. El Haj, R. Brown, V. Salih, J. Hilborn, S. Larsson, R.O.C. Oreffo, A surprisingly poor correlation between in vitro and in vivo testing of biomaterials for bone regeneration: Results of a multicentre analysis, 31 (2016) 312–322.

[11] L. Di Silvio, Cellular Response to Biomaterials, 2008. doi:10.1533/9781845695477.

[12] D.F. Williams, On the mechanisms of biocompatibility, Biomaterials. 29 (2008) 2941–2953. doi:10.1016/j.biomaterials.2008.04.023.

[13] S.L. Hirsh, D.R. McKenzie, N.J. Nosworthy, J.A. Denman, O.U. Sezerman, M.M.M. Bilek, The Vroman effect: Competitive protein exchange with dynamic multilayer protein aggregates, Colloids Surfaces B Biointerfaces. 103 (2013) 395–404. doi:10.1016/j.colsurfb.2012.10.039.

[14] G.S. Baht, L. Vi, B.A. Alman, The Role of the Immune Cells in Fracture Healing, Curr. Osteoporos. Rep. 16 (2018) 138–145. doi:10.1007/s11914-018-0423-2.

[15] B.J. Kwee, D.J. Mooney, Manipulating the Intersection of Angiogenesis and Inflammation, Ann. Biomed. Eng. (2015). doi:10.1007/s10439-014-1145-y.

[16] K.R. Fernandes, Y. Zhang, A.M.P. Magri, A.C.M. Renno, J.J.J.P. Van Den Beucken, Biomaterial Property Effects on Platelets and Macrophages: An in Vitro Study, ACS Biomater. Sci. Eng. (2017). doi:10.1021/acsbiomaterials.7b00679.

[17] Y. Zhang, X. Cheng, J.A. Jansen, F. Yang, J.J.J.P. van den Beucken, Titanium surfaces characteristics modulate macrophage polarization, Mater. Sci. Eng. C. (2018) #pagerange#. doi:10.1016/j.msec.2018.10.065.

[18] F.O. Martinez, S. Gordon, The M1 and M2 paradigm of macrophage activation: time for reassessment., F1000Prime Rep. 6 (2014) 13. doi:10.12703/P6-13.

[19] G.S.A. Boersema, N. Grotenhuis, Y. Bayon, J.F. Lange, Y.M. Bastiaansen-Jenniskens, The Effect of Biomaterials Used for Tissue Regeneration Purposes on Polarization of Macrophages., Biores. Open Access. 5 (2016) 6–14. doi:10.1089/biores.2015.0041.

[20] K.L. Spiller, R.R. Anfang, K.J. Spiller, J. Ng, K.R. Nakazawa, J.W. Daulton, G. Vunjak-Novakovic, The role of macrophage phenotype in vascularization of tissue engineering scaffolds, Biomaterials. (2014). doi:10.1016/j.biomaterials.2014.02.012.

[21] N. Araújo-Gomes, F. Romero-Gavilán, I. García-Arnáez, C. Martínez-Ramos, A.M. Sánchez-Pérez, M. Azkargorta, F. Elortza, J.J.M. de Llano, M. Gurruchaga, I. Goñi, J. Suay, Osseointegration mechanisms: a proteomic approach, J. Biol. Inorg. Chem. (2018) 1–12. doi:10.1007/s00775-018-1553-9.

[22] F. Romero-Gavilan, N. Araújo-Gomes, A.M. Sánchez-Pérez, I. García-Arnáez,

F. Elortza, M. Azkargorta, J.J.M. de Llano, C. Carda, M. Gurruchaga, J. Suay, I. Goñi, Bioactive potential of silica coatings and its effect on the adhesion of proteins to titanium implants, Colloids Surfaces B Biointerfaces. 162 (2018). doi:10.1016/j.colsurfb.2017.11.072.

[23] J.R. Wisniewski, A. Zougman, N. Nagaraj, M. Mann, J.R. Wi, Universal sample preparation method for proteome analysis, Nat. Methods. 6 (2009) 377–362. doi:10.1038/nmeth.1322.

[24] C. Maniatopoulos, A. Rodriguez, D.A. Deporter, A.H. Melcher, An improved method for preparing histological sections of metallic implants, Int. J. Oral Maxillofac. Implant. 1 (1986) 31–37.

[25] J. Yuste, M. Botto, S.E. Bottoms, J.S. Brown, Serum amyloid P aids complement-mediated immunity to Streptococcus pneumoniae, PLoS Pathog. 3 (2007) 1208–1219. doi:10.1371/journal.ppat.0030120.

[26] L.L. Hench, Third-Generation Biomedical Materials, Science (80-. ). 295 (2002) 1014–1017. doi:10.1126/science.1067404.

[27] L. Gabrielli, L. Russo, A. Poveda, J.R. Jones, F. Nicotra, J. Jiménez-Barbero, L. Cipolla, Epoxide opening versus silica condensation during sol-gel hybrid biomaterial synthesis, Chem. - A Eur. J. 19 (2013) 7856–7864. doi:10.1002/chem.201204326.

[28] E.M. Valliant, J.R. Jones, Softening bioactive glass for bone regeneration: sol–gel hybrid materials, Soft Matter. 7 (2011) 5083. doi:10.1039/c0sm01348j.

[29] J.M. Anderson, K. Defife, A. McNally, T. Collier, C. Jenney, Monocyte, macrophage and foreign body giant cell interactions with molecularly engineered surfaces., J. Mater. Sci. Mater. Med. (1999). doi:238415 [pii].

[30] A. John Gwinnett, F.R. Tay, Early and intermediate time response of the dental pulp to an acid etch technique in vivo, in: Am. J. Dent., 1998.

[31] C. Mold, H. Gewurz, T.W. Du Clos, Regulation of complement activation by C-reactive protein, in: Immunopharmacology, 1999: pp. 23–30. doi:10.1016/S0162-3109(99)00007-7.

[32] P. Garred, C. Honoré, Y.J. Ma, L. Munthe-Fog, T. Hummelshøj, MBL2, FCN1, FCN2 and FCN3-The genes behind the initiation of the lectin pathway of complement, Mol. Immunol. 46 (2009) 2737–2744. doi:10.1016/j.molimm.2009.05.005.

[33] P. Nesargikar, B. Spiller, R. Chavez, The complement system: History, pathways, cascade and inhibitors, Eur. J. Microbiol. Immunol. 2 (2012) 103–111. doi:10.1556/EuJMI.2.2012.2.2.

[34] J. Andersson, K.N. Ekdahl, J.D. Lambris, B. Nilsson, Binding of C3 fragments on

top of adsorbed plasma proteins during complement activation on a model biomaterial surface, Biomaterials. 26 (2005) 1477–1485. doi:10.1016/j.biomaterials.2004.05.011.

[35] F. Forneris, P. Gros, Chapter 630 - Complement Factor D, Handb. Proteolytic Enzym. 46 (2013) 2841–2848. doi:http://dx.doi.org/10.1016/B978-0-12-382219-2.00630-X.

[36] M.M. Frank, K.E. Sullivan, Deficiencies of the Complement System, in: Stiehm's Immune Defic., 2014: pp. 731–763. doi:10.1016/B978-0-12-405546-9.00038-8.

[37] F. Romero-Gavilán, N. Araújo-Gomes, I. García-Arnáez, C. Martínez-Ramos, F. Elortza, M. Azkargorta, I. Iloro, M. Gurruchaga, J. Suay, I. Goñi, The effect of strontium incorporation into sol-gel biomaterials on their protein adsorption and cell interactions, Colloids Surfaces B Biointerfaces. 174 (2019) 9–16. doi:10.1016/J.COLSURFB.2018.10.075.

[38] S. Devaraj, I. Jialal, C-reactive protein polarizes human macrophages to an M1 Phenotype and inhibits transformation to the M2 phenotype, Arterioscler. Thromb. Vasc. Biol. 31 (2011) 1397–1402. doi:10.1161/ATVBAHA.111.225508.

[39] K.L. Spiller, E.A. Wrona, S. Romero-Torres, I. Pallotta, P.L. Graney, C.E. Witherel, L.M. Panicker, R.A. Feldman, A.M. Urbanska, L. Santambrogio, G. Vunjak-Novakovic, D.O. Freytes, Differential gene expression in human, murine, and cell line-derived macrophages upon polarization, Exp. Cell Res. 347 (2016) 1–13. doi:10.1016/j.yexcr.2015.10.017.

[40] H. Chanteux, A.C. Guisset, C. Pilette, Y. Sibille, LPS induces IL-10 production by human alveolar macrophages via MAPKinases- and Sp1-dependent mechanisms, Respir. Res. 8 (2007) 1–10. doi:10.1186/1465-9921-8-71.

[41] R.A. Pengal, L.P. Ganesan, G. Wei, H. Fang, M.C. Ostrowski, S. Tridandapani, Lipopolysaccharide-induced production of interleukin-10 is promoted by the serine/threonine kinase Akt, Mol. Immunol. 43 (2006) 1557–1564. doi:10.1016/j.molimm.2005.09.022.

[42] M.S. Nanes, Tumor necrosis factor-α: Molecular and cellular mechanisms in skeletal pathology, Gene. 321 (2003) 1–15. doi:10.1016/S0378-1119(03)00841-2.

[43] X. Wu, W. Xu, X. Feng, Y. He, X. Liu, Y. Gao, S. Yang, Z. Shao, C. Yang, Z. Ye, TNF-a mediated inflammatory macrophage polarization contributes to the pathogenesis of steroid-induced osteonecrosis in mice, Int. J. Immunopathol. Pharmacol. 28 (2015) 351–361. doi:10.1177/0394632015593228.

[44] D. Mevorach, J.O. Mascarenhas, D. Gershov, K.B. Elkon, Complement-dependent clearance of apoptotic cells by human macrophages., J. Exp. Med.

188 (1998) 2313–2320. doi:10.1084/jem.188.12.2313.

[45] M.D. Galvan, M.C. Greenlee-Wacker, S.S. Bohlson, C1q and phagocytosis: the perfect complement to a good meal, J. Leukoc. Biol. 92 (2012) 489–497. doi:10.1189/jlb.0212099.

[46] S.S. Bohlson, S.D. O'Conner, H.J. Hulsebus, M.M. Ho, D.A. Fraser, Complement, C1Q, and C1q-related molecules regulate macrophage polarization, Front. Immunol. 5 (2014) 1–7. doi:10.3389/fimmu.2014.00402.

[47] E. Asgari, G. Le Friec, H. Yamamoto, E. Perucha, S.S. Sacks, J. Köhl, H.T. Cook, C. Kemper, C3a modulates IL-1β secretion in human monocytes by regulating ATP efflux and subsequent NLRP3 inflammasome activation, Blood. 122 (2013) 3473–3481. doi:10.1182/blood-2013-05-502229.

[48] E.O. Samstad, N. Niyonzima, S. Nymo, M.H. Aune, L. Ryan, S.S. Bakke, K.T. Lappegard, O.-L. Brekke, J.D. Lambris, J.K. Damas, E. Latz, T.E. Mollnes, T. Espevik, Cholesterol Crystals Induce Complement-Dependent Inflammasome Activation and Cytokine Release, J. Immunol. 192 (2014) 2837–2845. doi:10.4049/jimmunol.1302484.